LA-UR-98-1266

Approved for public release; distribution is unlimited.

TITLE: MECHANICAL PROPERTIES OF NITI-TIC SHAPE-MEMORY COMPOSITES

CONF-971201--

AUTHOR(S): M.A. Bourke, MST-5
J.A. Roberts, LANSCE 12

SUBMITTED TO: 1996 MRS Meeting

Los Alamos
NATIONAL LABORATORY

Form No. 836 R5
ST 2629 10/91

DISCLAIMER

to be printed in *Advances in Materials for Smart Systems* (MRS 1996 Fall Meeting).

MECHANICAL PROPERTIES OF NiTi-TiC SHAPE-MEMORY COMPOSITES

D.C. DUNAND*, K.L. FUKAMI-USHIRO¶, D. MARI#, J.A. ROBERTS§, M.A. BOURKE§
* Department of Materials Science and Engineering, Massachusetts Institute of Technology, Cambridge, MA 02139, ¶ Raychem Corp., Menlo Park CA 94025, # ACME, 1015 Lausanne, Switzerland, § LANSCE, Los Alamos National Laboratory, Los Alamos, NM 87545.

ABSTRACT

This paper reviews recent work on the mechanical behavior of martensitic NiTi composites reinforced with 10-20 vol.% TiC particulates. The behavior of the composites is compared to that of unreinforced NiTi, so as to elucidate the effect of mismatch due to matrix transformation, thermal expansion, twinning or slip, in the presence of purely elastic particles. The twinning and subsequent thermal recovery of deformed composites, measured both macroscopically (by compressive testing and by dilatometry) and microscopically (by neutron diffraction), are summarized.

INTRODUCTION

The intermetallic NiTi plays a central role in the area of smart materials, because it is capable of large scale recovery after deformation upon heating (i.e. the shape-memory effect) or upon mechanical unloading (i.e. the superelastic effect), depending on stoichiometry and temperature. Both these effects are the result of the allotropic nature of NiTi and its unusual deformation mechanisms which, unlike dislocation motion, are reversible: twinning (leading to shape-memory recovery by thermally-induced phase transformation) and stress-induced transformation (leading to superelastic recovery by a stress-induced back-transformation). Recently, there has been interest in NiTi-based composites with shape-memory capabilities. Most of the research has focused on imbedding NiTi wires or foils within an organic [1-4] or metallic [5, 6] matrix. On the other hand, we have investigated metal matrix composites with a martensitic NiTi matrix and inert ceramic particulates as a second phase, with the aim to examine the effect of mismatch stresses between matrix and reinforcement upon the deformation and subsequent shape-memory recovery of the composites. Since the allotropic transformation responsible for the unique properties of NiTi is thermoelastic, these mismatch stresses can be expected to strongly affect the mechanical response of the matrix.

This review summarizes recent work done at MIT in the area of mechanical properties of TiC-reinforced metal matrix composites with a martensitic NiTi matrix. More details can be found in the original articles describing the thermal transformation behavior [7, 8], the bulk mechanical properties in compression [9], the subsequent shape-memory recovery [10] and the study by neutron diffraction of twinning deformation and shape-memory recovery [11, 12].

EXPERIMENT

While the detailed experimental procedures can be found in the original publications [7-12], a brief summary is given in the following. Billets were fabricated by hot-pressing (followed in some cases by hot-isostatically pressing) of blended powders of prealloyed NiTi (51.4 at % Ti) and TiC particles (between 44 μm and 100 μm in size) with volume fractions 0%, 10% or 20%. Compression samples (respectively labeled in what follows NiTi, NiTi-10TiC and NiTi-20TiC) were cut from the billets by electro-discharge machining and annealed at 930 °C for 1 hour.

Mechanical testing was performed in compression between graphite-lubricated carbide plattens with strain measured by strain gauges, a linear variable displacement transducer or an extensometer. Specimens were thermally recovered in air in a Orton dilatometer outfitted with quartz sample-holder and push-rod. Heating occurred from 20°C to a maximum temperature of at least 275°C at a rate of 1 K/min., followed by cooling to 20°C at the same rate.

Neutron diffraction measurements were performed in time-of-flight mode at the pulsed neutron source of the Los Alamos Neutron Science Center. Two samples (*NiTi and NiTi-20TiC*) were deformed in compression up to a stress of -280 MPa, unloaded and subsequently recovered above A_f and cooled to room temperature. Strains parallel and perpendicular to the loading axis were calculated from the shift of individual Bragg reflections at a series of stress values, using two detectors forming an angle with respect to the incident beam of -90° (scattering vector Q parallel to the load) and +90° (Q perpendicular to the load). The unstressed, annealed bulk samples were used as a stress-free reference. Changes in the intensities of individual reflections, which correspond to changes in the fraction of NiTi variants in the diffraction condition, were quantified with a Normalized Scale Factor defined as the ratio of a peak intensities under load and prior to loading. The average material response was determined using the Rietveld approach, where the intensities and positions of all Bragg peaks are predicted from an assumed crystal structure.

RESULTS

Compression Behavior

A typical stress-strain curve for NiTi is shown in Fig. 1 with compressive stress and strain given as positive values. Phases are identified as follows: β denotes the austenitic parent phase: M refers to the annealed martensitic phase consisting of the 24 possible variants; and the deformed, twinned martensite is labeled M'. Dominant mechanisms can be separated by the five regimes shown in Fig. 1. On loading in Region A, the martensite M deforms elastically. Region B corresponds to deformation by twinning (M → M'). Deformation in Region C includes contributions of both Region B and Region D (elastic and plastic deformation by slip of oriented martensite M'). Finally, upon unloading in Region E, elastic recovery and some reverse twinning of oriented M' are responsible for strain recovery. Figure 2 shows the stress-strain curves of all samples deformed at room temperature far below M_f (M_f = 57-64 °C).

Shape-Memory Behavior

In dilatometric recovery experiments conducted on specimens deformed at room temperature, the recovery R was defined as:

$$R = \frac{L(T) - L_M(T)}{L_A(T) - L_M(T)} \qquad (1)$$

where L(T) is the measured length of the specimen as the temperature T, $L_A(T)$ is the length of the fully recovered austenitic sample and $L_M(T)$ is the hypothetical length of the deformed, unrecovered martensitic sample. Another recovery parameter directly comparable to the mechanical prestrain e_p is the recovery strain e, defined as:

$$e = \frac{L(T) - L_M(T)}{L_0} \qquad (2)$$

where L_0 is the initial specimen length.

Figure 3 depicts a typical dilatometry curve which can be separated in regions with different slopes. Some strain is recovered during initial heating of the deformed martensite M' in Region 1. The main recovery by the (M' → β) transformation is characterized by a large expansion in Region 2 between A_s and A_f, while limited post-transformation recovery takes place in Region 3, where most of the matrix consists of austenite. Upon cooling, negligible recovery is measured in Region 4, while the austenite β transforms back to martensite in Region 5 between M_s and M_f. The martensitic structure obtained after the first thermal recovery cycle is referred to as M", which is associated with a net contraction or expansion in Region 5, depending on the magnitude of the prestrain.

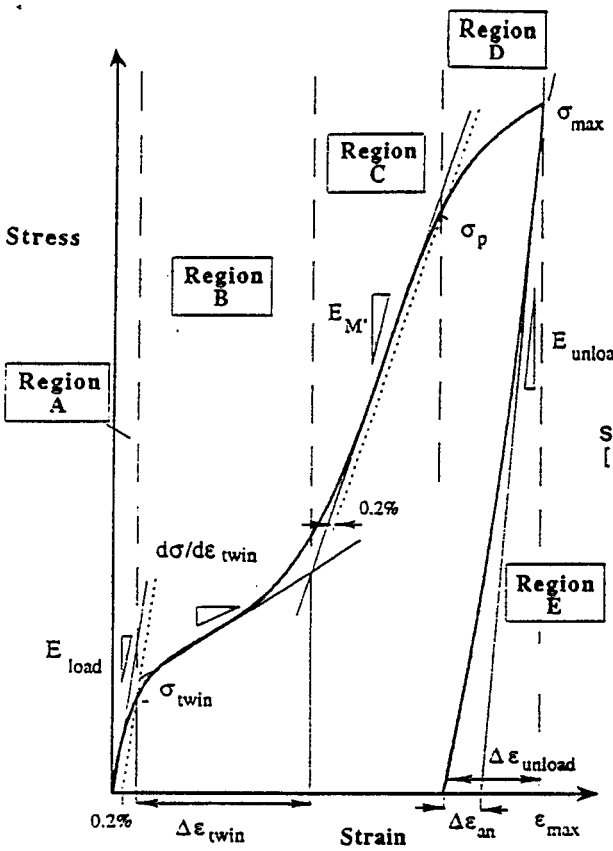

Fig. 1: Schematic compression stress-strain curve for NiTi

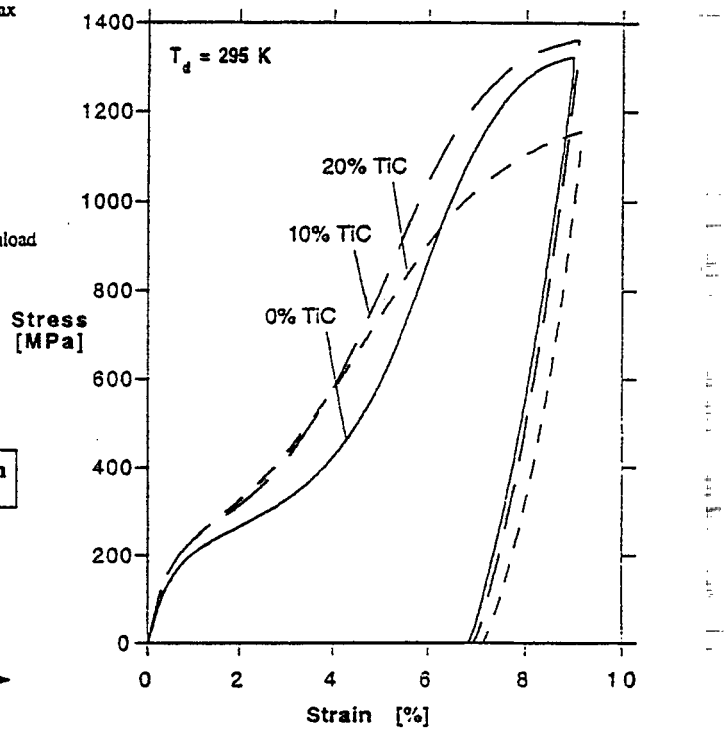

Fig. 2: Stress-strain curve of NiTi and NiTi-TiC composites at room temperature.

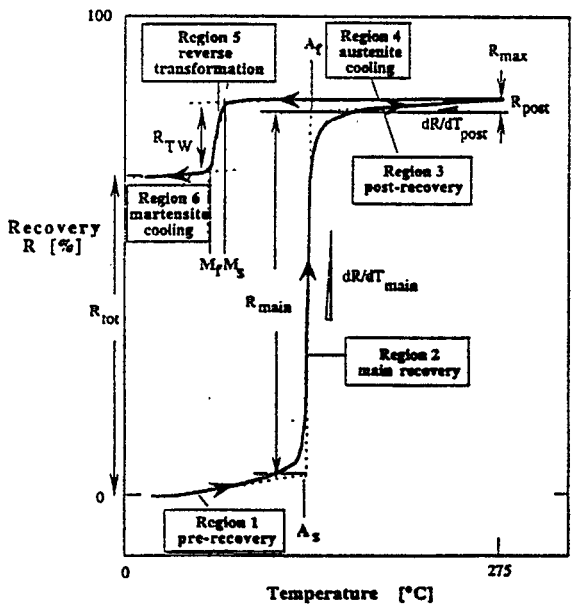

Fig. 3: Schematic dilatometry curve with its 6 main regions.

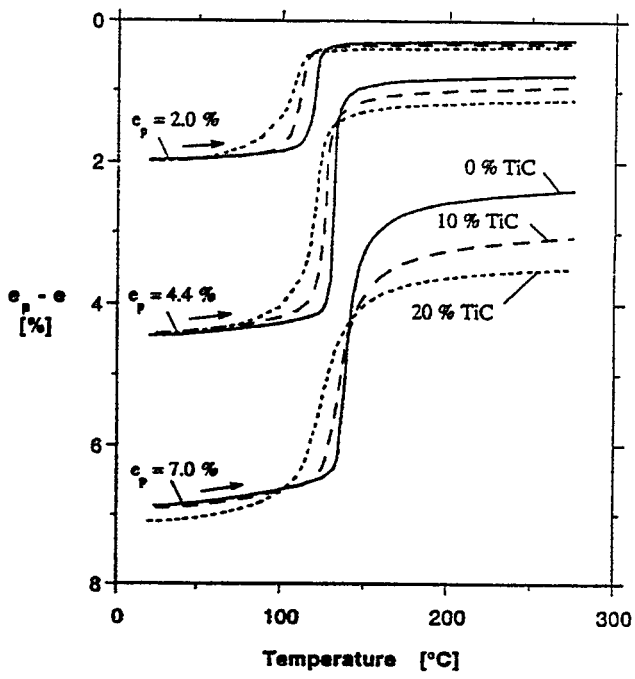

Fig. 4: Recovery strain upon heating of specimens deformed to various prestrains.

Figure 4 shows the strain recovered upon heating for samples deformed to three different mechanical prestrains. It is apparent that (i) with *increasing prestrain, the transformation* temperatures A_s and A_f increase, and recovery strain e increases while recovery extent R decreases; (ii) with increasing TiC volume fraction, recovery strain e and recovery extent R decrease, and transformation temperatures A_s and A_f decrease while the transformation temperature range $A_f - A_s$ increases.

In Fig. 5, the cooling behavior of NiTi-20%TiC is shown as a function of prestrain, with strains emanating from a value of 0% at a temperature of 100 °C for comparison purpose. The ($\beta \rightarrow$ M') recovery is negative for all non-zero prestrains, indicating the Two-Way Shape-Memory Effect (TWSME). A qualitatively similar behavior was found for NiTi-10%TiC and NiTi. However, compared to unreinforced NiTi, the composites exhibit lower transformation temperatures M_s and M_f, wider transformation temperature range $M_s - M_f$ and a smaller total strain recovery (Fig. 6) but larger TWSME strain (Fig. 7).

Neutron Diffraction

Figure 8 shows for NiTi-20TiC the residual strains for the most important planes under no applied stress after mechanical unloading and after shape-memory recovery. While the sign of the residual strains varies between these two states, their magnitude and average are similar. Also, residual strains for all measured planes are similar for NiTi and NiTi-20TiC. Figure 8 also shows the average residual strain after unloading and recovery, calculated as the mean of the residual strains in the three cell directions determined from crystallographic constants.

Figure 9 shows the normalized scale factors of the most intense reflections as a function of the plastic strain during loading. Because the scale factors are proportional to the integrated peak intensities, they are a measure of the volume fraction of variants with planes in the Bragg condition, and thus describe preferred orientation. The systematic increase or decrease of the scale factors indicates that a texture develops upon deformation as a result of twinning. The composite exhibits the same preferred orientation behavior as the bulk matrix, indicating that the TiC particles have only a small effect on the average twinning behavior of the matrix.

Upon unloading however, the scale factors of NiTi and NiTi-20TiC evolve quite differently, as depicted in Figs. 10 (a,b). Moreover, in contrast to loading (Fig. 9), there is upon unloading no linear relationship between scale factors and plastic strain: in many cases, the scale factor /plastic strain curves exhibit a change of slope sign, indicative of a complex twinning behavior. In most cases, however, a trend to reversion towards the undeformed state is observed for the scale factors upon shape memory recovery, but not in the reversible fashion suggested by the dotted line in Figs. 10 (a,b).

DISCUSSION

Compressive Behavior

Assuming that the TiC particles do not induce additional twinning in the matrix and that elastic load transfer from the matrix is operative, the composite stiffness tensor can be predicted by the Eshelby's theory [13]. With an apparent elastic modulus $E_M = 68$ GPa for NiTi (incorporating both elastic and twinning contributions in Region A), theory predicts for the composites the elastic modulus values given in Table I, which also lists the experimental values measured by strain gauge. For an experimental error estimated at about ±3 GPa, the measured elastic modulus for NiTi-10TiC is in agreement with predictions from the Eshelby theory. This shows that stiffening results from load transfer to the TiC particles without creation of mismatch stresses exceeding the critical stress for twinning σ_{twin}, which would induce significant additional matrix twinning and a lower apparent elastic modulus. However, the elastic modulus of NiTi-20TiC, is significantly smaller than predicted by the Eshelby theory, indicating that stiffening by load transfer to the TiC particles is partially canceled by the additional twinning resulting from relaxation of elastic incompatibility between matrix and reinforcement. Only a small twinning strain ε_t is needed to decrease the modulus from a theoretical value E = 94 GPa to an apparent macroscopic average

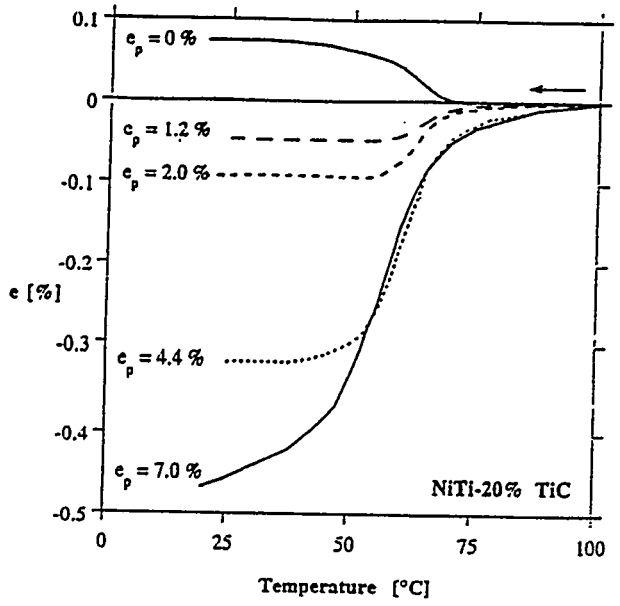

Fig. 5: Strain upon cooling of NiTi-20% TiC deformed to different prestrains.

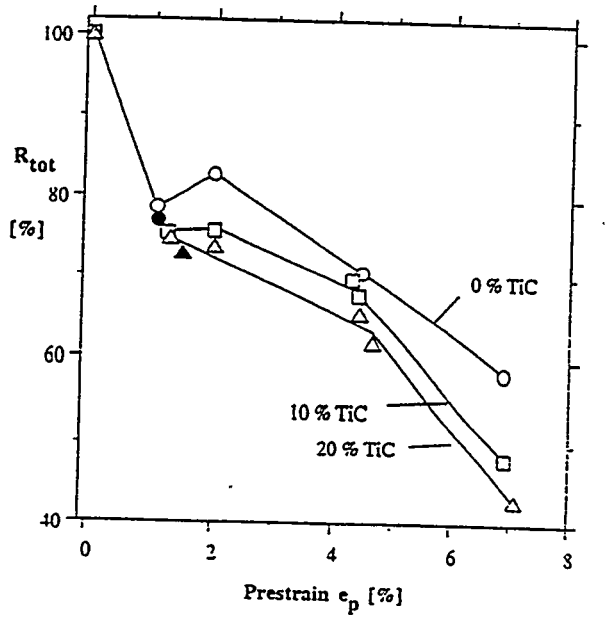

Fig. 6: Total extent of recovery after a full cycle as a function of prestrain.

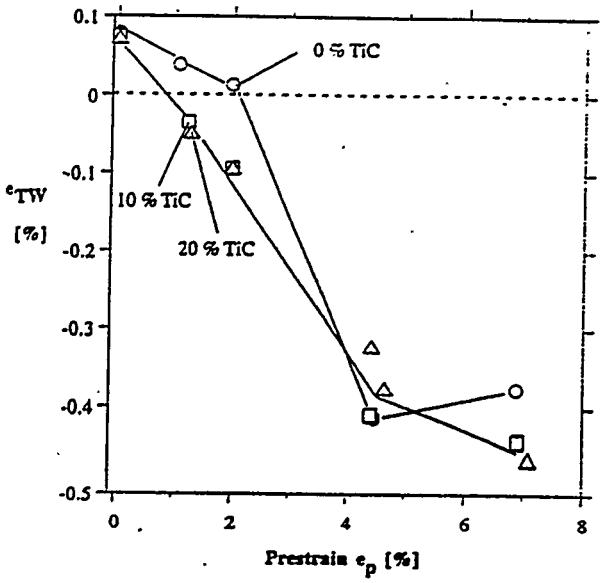

Fig. 7: TWSME recovery strain as a function of prestrain.

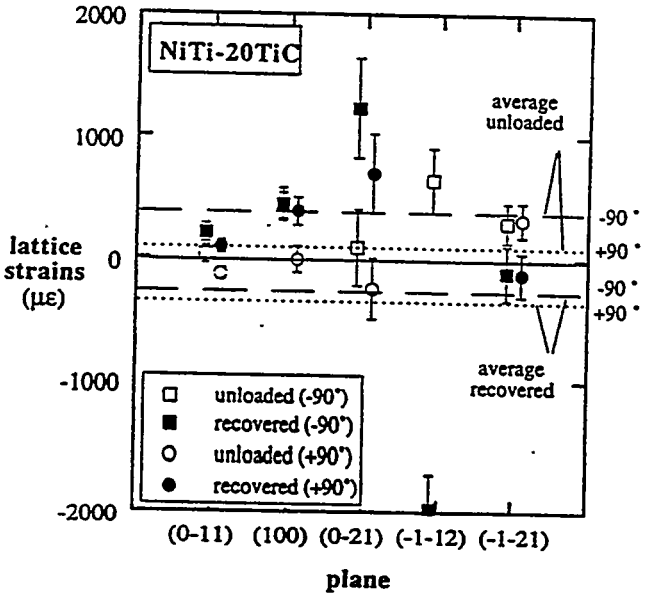

Fig. 8: Residual strain measured by neutron diffraction for NiTi-20TiC after mechanical unloading (empty symbols) and shape-memory recovery (filled symbols),with average values determined by Rietveld refinement.

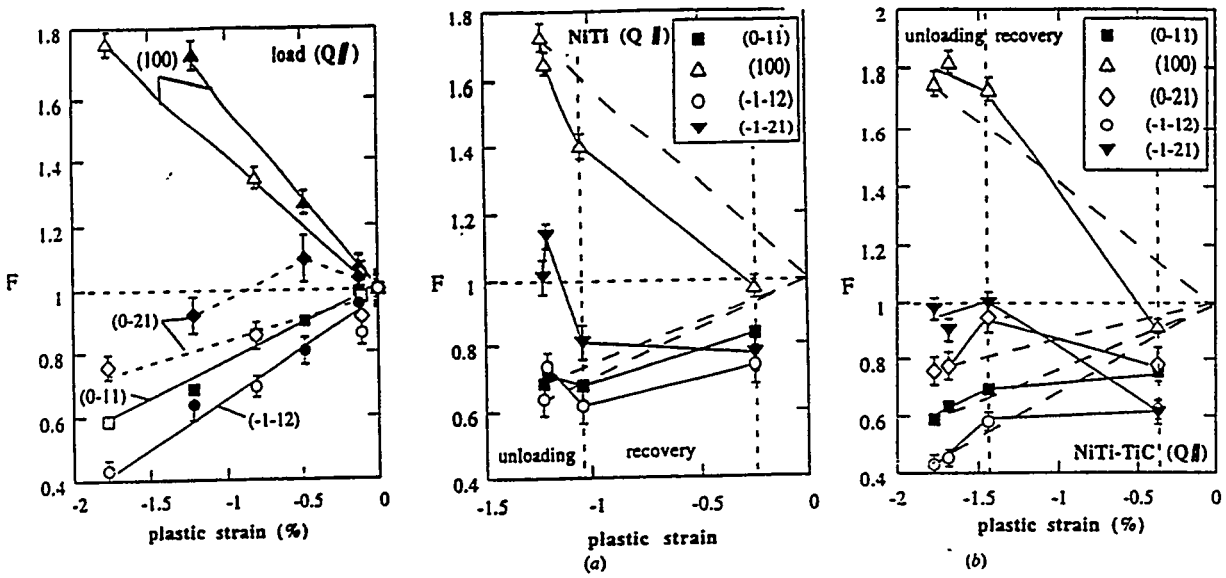

Fig. 9: Normalized scale factor upon mechanical loading as a function of plastic strain for NiTi (filled symbols) and NiTi-20TiC (empty symbols).

Fig. 10: Normalized scale factor upon mechanical unloading as a function of plastic strain
(a) NiTi
(b) NiTi-20TiC.

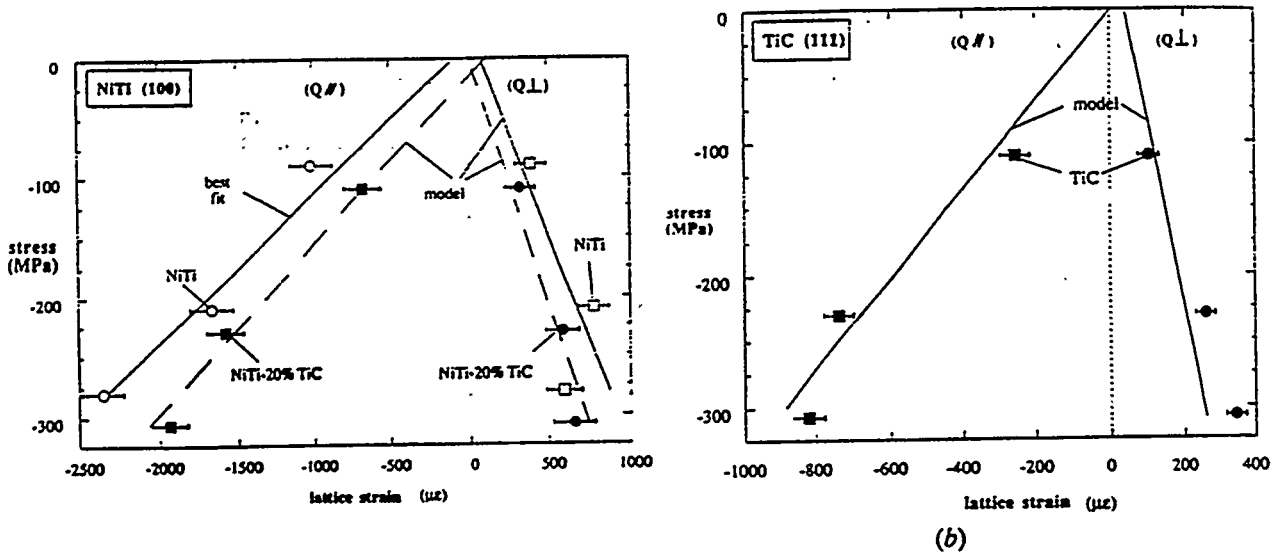

Fig. 11: Measured elastic gradients for (100) planes in both phases and both directions. The linear regression fits are shown as full lines and the predicted behavior from the Eshelby's method as dotted lines.
(a) NiTi lattice strains for NiTi and NiTi-20TiC (b) TiC lattice strains for NiTi-20TiC.

E_{app} = 79 GPa: for an applied stress $\sigma = -50$ MPa, corresponding to the apparent macroscopic yield stress, this strain is less than 0.02%. Early twinning in NiTi-20TiC is similar to the continuous yielding behavior observed in metal matrix composites deforming by slip. Upon application of a small external stress, the yield stress is reached internally as a result of the elastic mismatch between the two phases, resulting in a plastic zone around the particulates. Upon overlap of these plastic zones, the composite yields at an applied stress much lower than the yield stress of the unreinforced matrix, and it may exhibit little or no measurable elastic deformation. In NiTi composites, localized matrix twinning, relaxing mismatch strains developed around the stiff TiC particles will also lead to a low apparent elastic modulus at small strains. At large strains, localized twinning does not preclude load transfer from the compliant matrix to the stiff reinforcement,.

This load transfer can also be calculated by the Eshelby method [13] for the case of a matrix deforming by slip. Assuming that generalized yield in the composite occurs at an applied stress σ_{yc} for which the matrix average stress in the composite is equal to the yield stress of the unreinforced matrix, σ_y, strengthening is described by a parameter P :

$$\sigma_{yc} = \frac{\sigma_y}{P} \tag{3}$$

P can be calculated from the Tresca yield criterion [13]. For NiTi composites, the yield stress σ_y can be replaced by σ_{twin}, the stress for the onset of twinning. The measured twinning stress values in Table I confirms that additional twinning is taking place in the composites, because of relaxation by twinning of the mismatch stresses between matrix and particles. Indeed, the measured value σ_{twin} is independent of the volume fraction TiC, in disagreement with the prediction of Eq. (A2) based on load transfer without relaxation. This is in contrast to the behavior of the metal matrix composites deforming by slip, whereby mismatch relaxation by dislocation punching strengthen the matrix and results in yield stress values higher than predicted by Eq. (A2).

With increasing fractions of TiC particles, the curves exhibit the following trends: increase of $d\sigma/d\varepsilon_{twin}$, and decreases of Δe_{twin}, $E_{M'}$ and σ_p. These observations can be explained by the stabilization of martensite M, as TiC particles prevent twinning (M $\rightarrow$ M') at strains above about 2%. Because twinning is inhibited by dislocations exerting a friction stress on the moving twin boundaries [14], dislocations created to accommodate the plastic mismatch between the matrix and reinforcement are expected to stabilize the martensitic matrix M. Finally, the significant decrease of the slip yield stress σ_p exhibited by NiTi-20TiC can be understood if the yield stress for plastic deformation by slip of M, which exists in larger quantities in NiTi-20TiC, is lower than that of M'. This suggests that twinning of M, which also produces dislocations in the product M', induces subsequent hardening upon plastic deformation by slip of M'.

Table I: Elastic modulus upon loading E_{load} and critical stress for the onset of twinning σ_{twin}, averaged for samples tested at room temperature with strain gauges.

	E_{load} (GPa)		σ_{twin} (MPa)	
	measured	predicted (Eshelby)	measured	predicted (Eq. 3)
NiTi	68	68*	180	180*
NiTi-10TiC	78	80	180	197
NiTi-20TiC	79	94	186	215

* assumed equal to the measured value

Shape-Memory Recovery

Mechanical strain in martensitic NiTi can be separated in three components: (i) plastic strain by twinning which is recoverable, (ii) plastic strain by slip which is unrecoverable and (iii) residual elastic strains, which do not on average contribute to the total macroscopic prestrain, but may be recovered by relaxation during phase transformation. These three types of strains affect the kinetics and thermodynamics of the transformation as follows: (i) twinning reduces the number of martensitic variants, thus facilitating their subsequent transformation to austenite, and may also induce residual elastic stresses, due to residual mismatch strains between twinned variants; (ii) dislocations introduced by slip both stabilize the deformed martensite and induce the TWSME by their elastic stress field; and (iii) elastic stresses stabilize the martensite, as described by the Clausius-Clapeyron equation, and can also induce the TWSME.

Figure 6 shows that the magnitude of the recovery R after a complete thermal cycle is significantly less than 100% for all materials. Incomplete recovery of about 50% was also reported by Johnson et al. [15] for NiTi samples fabricated by powder metallurgy after tensile prestrains of 2 to 10%. The lack of complete recovery after a complete cycle in our samples is not due to the TWSME, because the recovery at the maximum temperature is at most about 85 %. It thus appears that, upon compressive deformation, substantial unrecoverable deformation by slip occurs concurrently with recoverable deformation by twinning, even for prestrains as low as 1.2 %. Plastic deformation by slip represents about 15 % of the total plastic deformation for prestrain values e_p between 1% and 4.4%, i.e. in a regime where twinning is expected to be the dominant deformation mechanism (Fig. 2).

The mismatch between the NiTi matrix and the purely elastic TiC particles cannot be relaxed by the reinforcement, provided it does not fracture in the bulk or at the interface. However, relaxation of the elastic and plastic mismatches between the two phases may occur by twinning or slip of the matrix. In the first case, thermal transformation of mismatch twins formed during mechanical deformation to accommodate the elastic particles is similar to thermal transformation of twins responsible for the overall shape change of the specimen. Thus, the overall shape-memory recovery behavior of the composite is expected to differ little from that of the unreinforced matrix. In the second case, where matrix slip relaxed the mismatch with the reinforcement, dislocations are expected to stabilize the deformed martensite and enhance the TWSME. Furthermore, if relaxation by slip or twinning is incomplete after deformation, the resulting residual elastic stresses are also expected to affect the macroscopic recovery behavior by stabilizing the martensite and by inducing the TWSME. Residual elastic stresses after deformation, however, are small on average as measured by neutron diffraction (Fig. 8).

The effect of TiC particles can now be discussed in light of the mechanisms described above. First, enhanced slip deformation of the matrix to accommodate the mismatching particles can explain the following observations:

(i) With increasing TiC content, the extent of recovery R_{max} decreases for prestrains larger than e_p = 1.4%. This indicates that unrecoverable deformation by slip increases in the composites.

(ii) The strain recovery during the pre- and post-transformation (Regions 1 and 3, Fig. 3) increases with increasing TiC fractions, and the recovery gradient de/dT_{main} during the main recovery in Region 2 decreases. These two phenomena broaden the recovery temperature interval, as expected if the martensitic variants close to the particles contain more mismatch dislocations (and are thus more stabilized) than the variants far from the particles.

(iii) The TWSME strain increases with increasing TiC content (Fig. 7), as expected if the composites contain more dislocations, the elastic stress field of which biases the formation of oriented martensite.

Second, stored elastic stresses can explain the following observations:

(iv) All transformation temperatures A_s, A_f, M_s, and M_f decrease with increasing TiC content, in agreement with the effect of elastic stresses on a thermoelastic transformation [16].

(v) The TWSME strain increases with increasing TiC content (Fig. 7). While this effect can be explained by plastic deformation (see (iii) above), elastic stresses due to incomplete relaxation in the composite can also have the same effect.

We note that plastic deformation in the composites lowers the total extent of recovery after a full cycle R_{tot} (Fig. 6) by decreasing the magnitude of the recoverable plastic strain by slip (effect (i)) and by increasing the magnitude of the TWSME strain (effect (iii) or (v)).

We thus conclude that all the trends observed in the recovery characteristics of the composites can be explained by an increase in plastic strains in the matrix and increased residual elastic stresses due to the mismatch between the matrix and the reinforcement during compressive deformation. In most cases, however, the difference in recovery properties between reinforced and unreinforced NiTi is relatively minor, indicating that most of the mismatch is accommodated by twinning. These conclusions are similar to those drawn from the shape of the stress-strain curves, as discussed earlier.

Neutron Diffraction

As for any metal matrix composite cooled from an elevated processing temperature, NiTi-20TiC is expected to exhibit residual thermal mismatch stresses due to the mismatch in coefficients of thermal expansion between reinforcement and matrix. Furthermore, additional mismatch stresses are expected due to the allotropic transformation of NiTi. These thermal and allotropic mismatch contributions calculated by the Eshelby method are given in Table II at room temperature for both phases. The expansion of the matrix upon allotropic transformation, results in room-temperature residual strains smaller by about 30% than if no transformation had taken place (Table II). We thus conclude that the residual strains are virtually the same in the undeformed NiTi and the undeformed NiTi-20TiC, since the value of the average matrix strain due to phase mismatch in the composite ($\varepsilon = 1.28 \cdot 10^{-4}$, Table II) is on the order of the diffraction measurement accuracy.

Fig. 11 (a) shows for NiTi-20TiC the elastic behavior of the (100) planes, for which the measurement error is small and whose elastic gradient can be assimilated to $1/S_{11}$. For both directions parallel and perpendicular to the applied load, good agreement is found between the measured diffraction data and the elastic behavior of the matrix predicted from load transfer by the Eshelby theory. The matrix lattice strain for the highest applied stress seems to be slightly lower than expected if elastic load transfer were solely taking place. This indicates that additional load transfer may be taking place, as discussed later. Fig. 11 (b) shows the predictions for the TiC phase in the NiTi-20TiC sample, which are also in satisfactory agreement with diffraction measurement. We thus conclude that, while elastic load transfer is taking place in the NiTi-20TiC composite in quantitative agreement with predictions by the Eshelby theory (Figs. 11(a, b)), no macroscopic stiffening is observed in the apparent elastic region of the stress-strain plot, as described earlier, because of the enhanced matrix twinning needed to relax the mismatching particles.

Plastic deformation of the matrix in the presence of elastic particles results in a plastic mismatch which is additive to the elastic mismatch contribution. Thus, load transfer should be enhanced compared to a case where both phases are elastic, with a concomitant increase in the gradient of the applied stress versus the lattice strain curve of the matrix (Fig. 11a). Respectively

Table II: Predicted mean internal stress $\bar{\sigma}$ and mean internal strain $\bar{\varepsilon}$ for NiTi (matrix M) and TiC (inclusion I) at room temperature due to thermal mismatch and transformation mismatch between the two phases of NiTi-20TiC.

	$\bar{\sigma}_M$ (MPa)	$\bar{\sigma}_I$ (MPa)	$\bar{\varepsilon}_M$ ($\cdot 10^6$)	$\bar{\varepsilon}_I$ ($\cdot 10^6$)
thermal mismatch	75	-302	182	-416
transformation mismatch	-22	89	-54	123
total mismatch	53	-213	128	-293

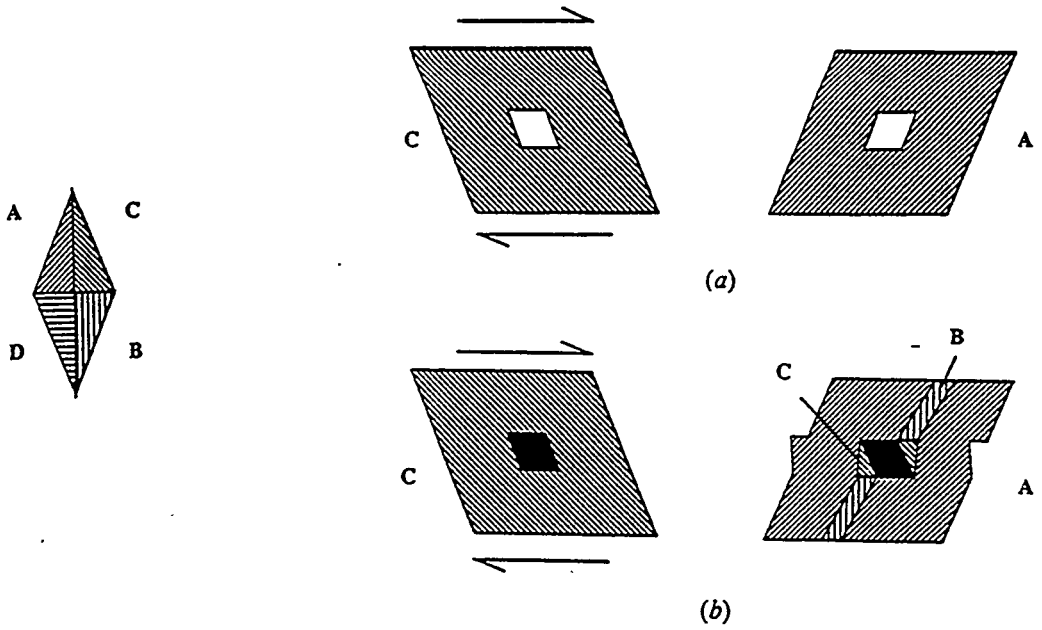

Fig. 12: Two-dimensional illustration of the accommodation of a mismatching rigid particle within a martensitic crystal with 4 possible variants.
(a) crystal with orientation C containing a hole, deformed by twinning to orientation A;
(b) crystal with orientation C containing a rigid particle, deformed by twinning to orientation A with accommodation twins C and B for the undeformed particle.

a decrease is expected for the elastic gradient of the reinforcement. These effects were observed by neutron diffraction in aluminum matrix composites deforming plastically by slip [13]. In the case of NiTi-20TiC deforming by twinning, these effects are much less than predicted by theory (Fig. 11), indicating that, unlike composites deforming by slip, NiTi-20TiC deforming by twinning relaxes very efficiently the plastic mismatch between matrix and reinforcement.

The *in-situ* neutron elastic and orientation measurements (Figs. 9 and 11) all indicate that the addition of 20 vol.% TiC particles has little effect on the plastic behavior of the matrix over the strain range explored here. This is in contrast with the increased strengthening, rate of strain hardening and plastic load transfer between matrix and reinforcement observed in metal matrix composites with a matrix plastically deforming by slip [13]. This insensitivity of the NiTi matrix to the presence of a large volume fraction of stiff, mismatching particles can be interpreted as the result of the greater ease, as compared to slip, for mismatch relaxation by twinning. When accommodation takes place by dislocation punching, strain hardening of the matrix and concomitant increase in strength result [17]. In contrast, complete relaxation of the mismatch between the elastic particle and the plastic matrix is possible by local twinning in martensitic NiTi composites. This is illustrated schematically in Fig. 12, for an hypothetical two-dimensional crystal with 4 possible variants. If the crystal contains a hole and is deformed by twinning from variant C to variant A, a concomitant change in the shape of the hole results. However, if the hole contains a rigid particle and the crystal is again twinned from variant C to variant A, complete accommodation of the resulting mismatch is possible by retaining some of the variant C in contact with the particle and accommodating the A-C boundary by a B twin (Fig. 12(b)). The net result is an overall macroscopic deformation similar to that of the particle-free case (Fig. 12(a)), with a small volume fraction of accommodating variants (B and C in Fig. 12 (b)). Because such accommodating variants are expected to also exist for particle-free, polycrystalline NiTi to relax mismatch between grains of different orientations, the twins necessary to accommodate elastic particles in a polycrystalline composite sample may represent only a small fraction of the twins already existing in particle-free polycrystalline samples. This hypothesis explains the lack of significant difference between NiTi and NiTi-20TiC in terms of macroscopic behavior and

average variant orientation by twinning (Fig. 9). Furthermore, unlike relaxation by slip, no strain hardening is expected as a result of localized twinning relaxing the mismatch.

TiC particles do not significantly interfere with the shape-memory effect for prestrains less than about 4%, corresponding to deformation by twinning. First, the fraction of strain recovered by shape-memory heat-treatment is only slightly smaller for NiTi-20TiC than for NiTi, as shown in Fig 6. This result confirms that the mismatching TiC particles do not induce a significant amount of slip in the material during deformation, since the strain resulting from slip is unrecoverable. Second, comparison of Figs. 10 (a,b) indicates that the preferred variant orientation after shape memory recovery is similar for both materials, despite the differences in variant orientation before shape-memory recovery. Third, the residual strains for all planes are, within experimental error, the same for both materials. If martensite deformation occurs purely by twinning of variants, which also accommodates the mismatch of TiC particles as depicted in Fig. 12, thermal transformation to austenite after twinning is indeed expected to be mostly unaffected by the TiC particles. Upon heating to a temperature above A_f, the composite is returned to the same state as before deformation, for which little thermal mismatch strains are expected (Table II). Subsequent cooling to room-temperature induces again small transformation mismatch strains, which can be minimized by self-accommodation through an appropriate combination of variants at the interface, similarly to the case of strain-induced deformation illustrated in Fig. 12(b).

SUMMARY

This paper gives an overview of recent work performed on martensitic NiTi composites containing 0, 10 and 20 vol.% TiC particulates. Mechanical deformation by twinning and subsequent strain recovery by shape-memory heat-treatment are investigated both macroscopically (by mechanical testing and by dilatometry) and microscopically (by neutron diffraction). The mismatch stresses between the elastic TiC particulate and the NiTi matrix due to matrix transformation and thermal expansion (during thermal excursions) and due to matrix twinning or slip (during mechanical deformation) are discussed.

ACKNOWLEDGMENTS

The work summarized in this paper was performed at MIT (with the financial support of the NSF Materials Research Laboratory, grant DMR90-22933, administrated through MIT's Center for Materials Science and Engineering) and at the Los Alamos Neutron Science Center (supported in part by DOE contract W-7405-ENG-36). DCD also gratefully acknowledges financial support by Daimler Benz Research and Technology and helpful discussions with Mr. Heinz Voggenreiter from that company.

REFERENCES

1. C.A. Rogers, C. Liang, and J. Jia, Comput. Struct. **38**, p. 569 (1991).

2. E. Hornbogen, M. Thumann, and B. Velten, in Progress in Shape Memory Alloys, edited by S. Eucken (DGM, Oberursel, Germany, City, 1992), p. 225.

3. J. Ro and A. Baz, Composite Eng. **5**, p. 61 (1995).

4. J.E. Bidaux, J.A. Manson, and R. Gotthardt, in First International Conference on Shape Memory and Superelastic Technologies, edited by A.R. Pelton, D. Hodgson, and T. Duerig (MIAS, Monterey CA, City, 1995), p. 37.

5. Y. Furuya, A. Sasaki, and M. Taya, Mater. Trans. JIM **34**, p. 224 (1993).

6. Y. Yamada, M. Taya, and R. Watanabe, Mater. Trans. JIM **34**, p. 254 (1993).

7. D. Mari and D.C. Dunand, Metall. Mater. Trans. **26A**, p. 2833 (1995).

8. D. Mari, L. Bataillard, D.C. Dunand, and R. Gotthardt, J. Physique IV **5**, p. 659 (1995).

9. K.L. Fukami-Ushiro and D.C. Dunand, Metall. Mater. Trans. **27A**, p. 183 (1996).

10. K.L. Fukami-Ushiro, D. Mari, and D.C. Dunand, Metall. Mater. Trans. **27A**, p. 193 (1996).

11. D.C. Dunand, D. Mari, M.A.M. Bourke, and J.A. Goldstone, J. Physique IV **5**, p. 653 (1995).

12. D.C. Dunand, D. Mari, M.A.M. Bourke, and J.A. Roberts, Metall. Mater. Trans. **27A**, p. 2820 (1996).

13. T.W. Clyne and P.J. Withers, An Introduction to Metal Matrix Composites, Cambridge University Press, Cambridge, 1993.

14. S. Miyazaki and K. Otsuka, Metall. Trans. **17A**, p. 53 (1986).

15. W.A. Johnson, J.A. Domingue, S.H. Reichman, and F.E. Sczerzenie, J. Physique **43**, p. C4 (1982).

16. R.J. Salzbrenner and M. Cohen, Acta Metall. **27**, p. 739 (1979).

17. M.F. Ashby, Phil. Mag. **21**, p. 399 (1970).